

# Appendix to

# The Dominant Role of Expectations and Broad-Based Supply Shocks in Driving Inflation

Paul Beaudry, Chenyu Hou and Franck Portier

April 2024

version 2.2

## **A Relation to Benigno and Eggertsson [2023]**

In this appendix, we repeat the analysis of section 1 when we use  $\log(V/U)$  as a measure of labour market tightness and either the Survey of Professional Forecasters (SPF) or the Michigan Survey of Consumers (MSC) as a measure of inflation expectations. We first stay with our baseline sample 1969-2007 where we use the expected GDP Deflator from the Professional Forecaster as our measure of expected inflation. We then move to the sample used in Benigno and Eggertsson [2023] (but stopping in 2007 to perform our out-of-sample analysis).

### **A.1 Sample 1969-2007**

Table A.1: Estimated Phillips Curves using  $\log(V/U)$  as a Measure of the Gap, 1969-2007

	Using SPF	Using MSC
$\beta$	1.26*	0.99*
	(0.047)	(0.048)
$\gamma_g$	0.28*	0.10
	(0.062)	(0.069)
$\gamma_r$	-0.42*	0.23*
	(0.098)	(0.040)
Observations	144	144
J Test	10.538	10.700
(jp)	(0.987)	(0.986)
Weak ID Test	29.469	10.201

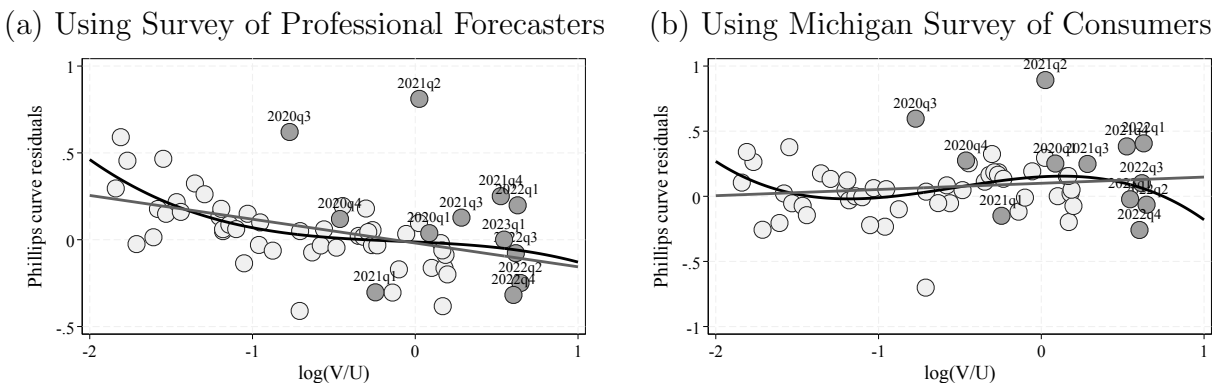
Notes: this table reports estimates of the augmented Phillips curve (2). All results are using IV-GMM procedure, Newey-West HAC standard errors with six lags are reported in parentheses. The constant term is omitted from the table. The measure of inflation is Core CPI and the gap is measured with  $\log(V/U)$ . All regressors are instrumented using six lags of Romer and Romer's [2004] shocks (as extended by Wieland and Yang [2020]) and their squares as instruments. A \* indicates significance at 5%. Sample is 1969Q1-2007Q4.

Table A.2: Projection of the Philips Curve Residuals  $\epsilon$  on the Gap  $\log(V/U)$ , 2008-2023

	Using SPF		Using MSC	
	linear	nonlinear	linear	nonlinear
$\log(V/U)$	-0.14*	-0.04	0.05	0.07
	(0.038)	(0.076)	(0.042)	(0.083)
$\log(V/U)^2$		-0.02		-0.25
		(0.149)		(0.162)
$\log(V/U)^3$		-0.06		-0.15*
		(0.082)		(0.089)
$N$	60	60	60	60
$\sigma_\epsilon$ 60-07		.302		.291
$\sigma_\epsilon$ 08-23		.232		.232

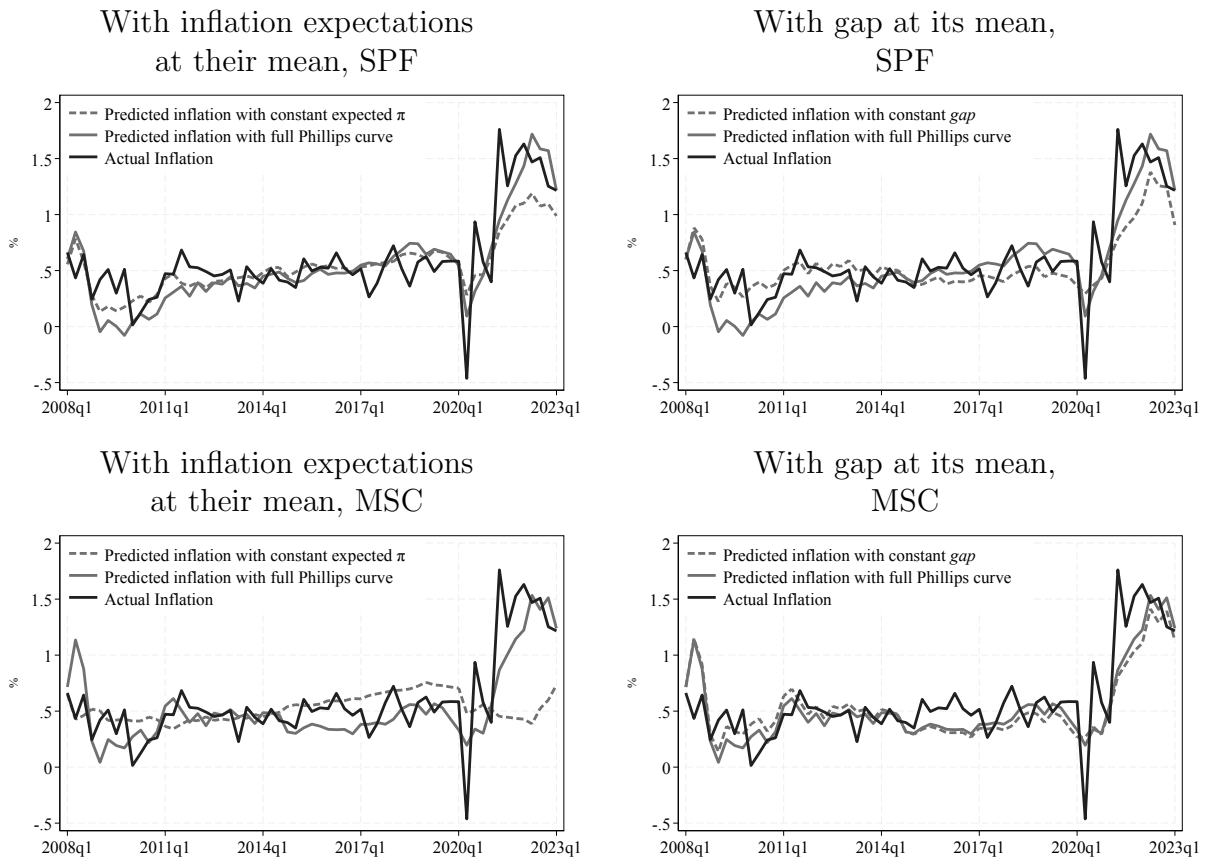
Notes: the Phillips curve residuals are obtained from the augmented Phillips curve (2) estimated over the sample 1969Q1-2007Q4, using  $\log(V/U)$  as a measure of the gap and either Survey of Professional Forecasters or Michigan Survey of Consumers as a measure of expectations. The standard errors of estimated coefficients are between parentheses.

Figure A.1: Out-of-Sample Residuals from Phillips Curve, using  $\log(V/U)$  as a Measure of the Gap



Notes: Panels (a) and (b) of this figure plots the out-of-sample residuals of the estimated Phillips curve (2) against  $\log(V/U)$  as the measure of labor market tightness, for two measures of inflation expectations. The gray lines show the estimated linear or cubic relation between residuals and labor market tightness (see Table A.2 for the estimated coefficients). Light dots correspond to pre-2020 observations and dark ones to post-2020. We exclude 2020q2 from this graph.

Figure A.2: Counterfactual Simulations from the Estimated Phillips Curve



Notes: These counterfactual simulations are done using the estimated Phillips curve (2), using  $\log(V/U)$  as the measure of labor market tightness.

## A.2 Sample 1981-2007

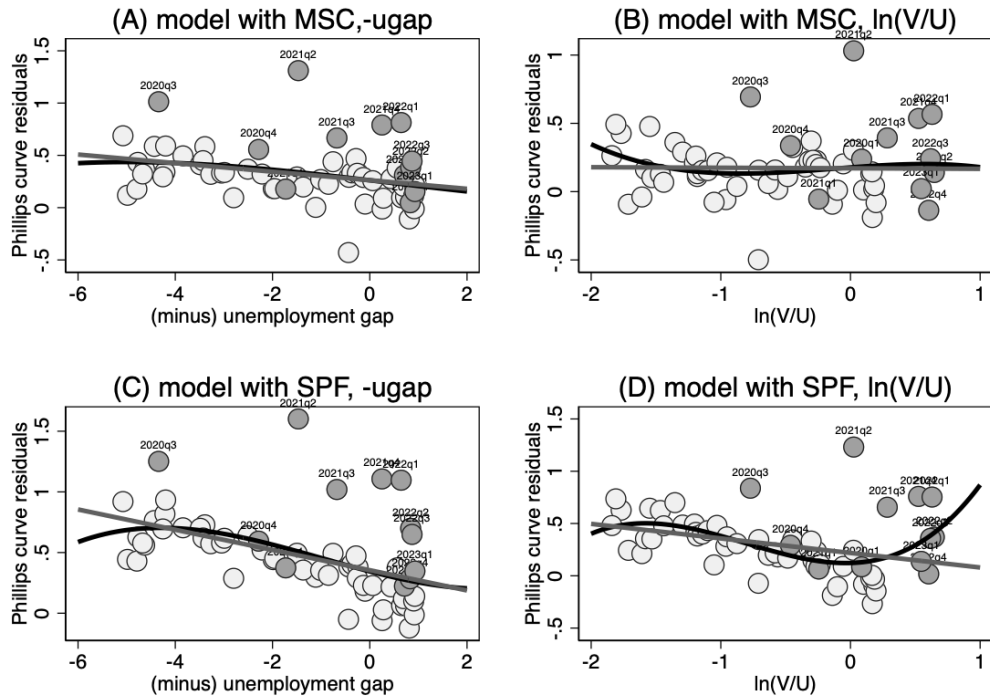
We then move to use the expected CPI series from the Survey of Professional Forecasters. Because that series starts only after 1981 quarter 3, we use the sample 1981q3-2007q4 for our analysis. In Table A.3 we present the estimation results of our Phillips Curve. For comparison, we also include the estimates using *minus* unemployment gap as measure of labor market tightness in this shorter sample.

Table A.3: Estimated Phillips Curves using  $\log(V/U)$  as a Measure of the Gap, 1981-2007

Expectations:	Using MSC		Using SPF	
Labor Market Tightness:	(1) -ugap	(2) $\ln V/U$	(3) -ugap	(4) $\ln V/U$
$\beta$	0.90*	0.90*	0.97*	0.95*
	(0.033)	(0.033)	(0.048)	(0.045)
$\gamma_g$	0.07*	0.17*	0.10*	0.29*
	(0.019)	(0.071)	(0.017)	(0.070)
$\gamma_r$	0.35*	0.29*	0.33*	0.26*
	(0.052)	(0.049)	(0.065)	(0.067)
Observations	106	106	106	106
J Test	10.687	10.763	10.952	10.872
(jp)	(0.986)	(0.985)	(0.984)	(0.984)
Weak ID Test	163.460	60.640	121.279	89.040

Notes: this table reports estimates of the augmented Phillips curve (2). All results are using IV-GMM procedure, Newey-West HAC standard errors with six lags are reported in parentheses. The constant term is omitted from the table. The measure of inflation is Core CPI and the gap is measured with  $\log(V/U)$ . All regressors are instrumented using six lags of Romer and Romer's [2004] shocks (as extended by Wieland and Yang [2020]) and their squares as instruments. A \* indicates significance at 5%. Sample is 1981Q3-2007Q4.

Figure A.3: Out-of-Sample Residuals from Phillips Curve, 1981-2007



Notes: Panels (a) and (c) of this figure plots the out-of-sample residuals of the estimated Phillips curve (2) against minus unemployment gap as the measure of labor market tightness, for two measures of inflation expectations. Panels (b) and (d) of this figure plots the out-of-sample residuals against  $\ln(V/U)$  as the measure of labor market tightness, for two measures of inflation expectations. The gray lines show the estimated linear or cubic relation between residuals and labor market tightness (see Table A.4 for the estimated coefficients). Light dots correspond to pre-2020 observations and dark ones to post-2020. We exclude 2020q2 from this graph.

Table A.4: Projection of the Phillips Curve Residuals  $\epsilon$  on measures of gap, 2008-2023

Expectations:	MSC				SPF			
Gap:	-ugap		$\ln V/U$		-ugap		$\ln V/U$	
	(1)	(2)	(3)	(4)	(5)	(6)	(7)	(8)
$\text{gap}_t$	-0.04*	-0.05	-0.00	0.07	-0.08*	-0.10	-0.14*	0.04
	(0.017)	(0.057)	(0.042)	(0.084)	(0.019)	(0.065)	(0.048)	(0.091)
$\text{gap}_t^2$		-0.00		-0.02		0.01		0.50*
		(0.044)		(0.165)		(0.050)		(0.179)
$\text{gap}_t^3$		0.00		-0.05		0.00		0.21*
		(0.007)		(0.090)		(0.008)		(0.098)
Observations	60	60	60	60	60	60	60	60

*Notes: the Phillips curve residuals are obtained from the augmented Phillips curve (2) estimated over the sample 1981Q3-2007Q4, using  $-\text{ugap}$  or  $\log(V/U)$  as a measure of the gap and either Survey of Professional Forecasters or Michigan Survey of Consumers as a measure of expectations. The standard errors of estimated coefficients are between parentheses.*

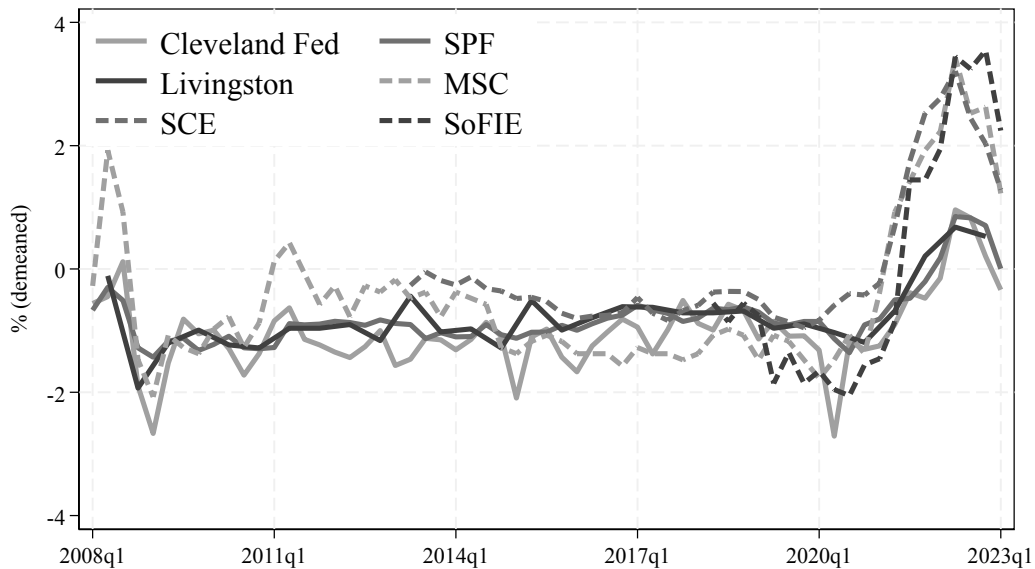
From the above analysis, we see only one specification suggests the Phillips Curve appears to become steeper in recent years. That is when using  $\ln V/U$  as a measure of labor market tightness, SPF as the measure of expected inflation and sample 1981Q3-2007Q4. Once we use the Michigan Survey of Consumers as the measure of expected inflation, such a pattern disappears. This is not surprising given the differences between the expected inflations from the survey of professionals and central banks, and those from the households and firms. In Appendix B we show the differences between various surveys of expectations and repeat our analysis with them.

## B Baseline Phillips Curve with Various Measures of Inflation Expectations

We first show the differences between various surveys of expectations. Figure B.1 depicts the demeaned series of expected inflation from different surveys. A stark pattern is that households and firms have similar expectations of inflation that are drastically different from

those of professional and central banks. In particular, the households and firms expect much higher inflation after 2020.

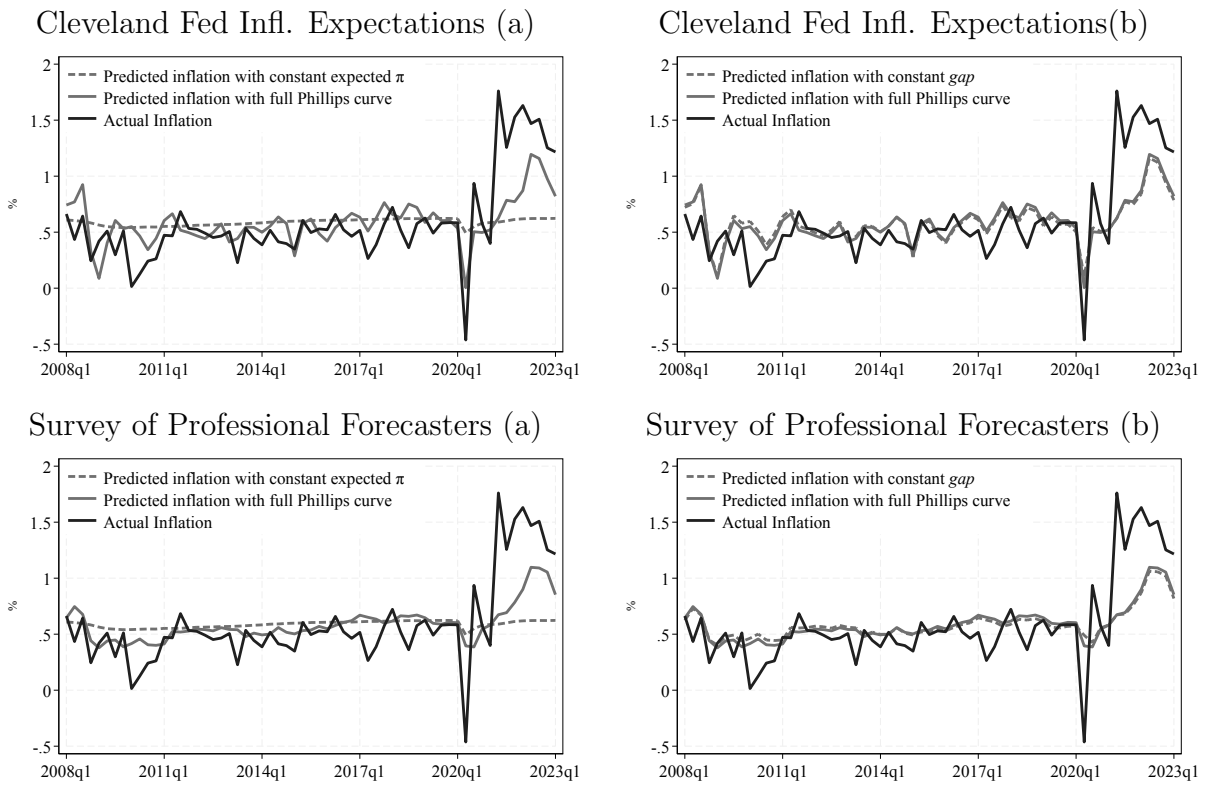
Figure B.1: Different measures of inflation expectations



*Notes: Demeaned average expected inflation from various surveys. Solid lines are from the surveys of professionals and central banks. The dashed lines are from surveys of households and firms.*

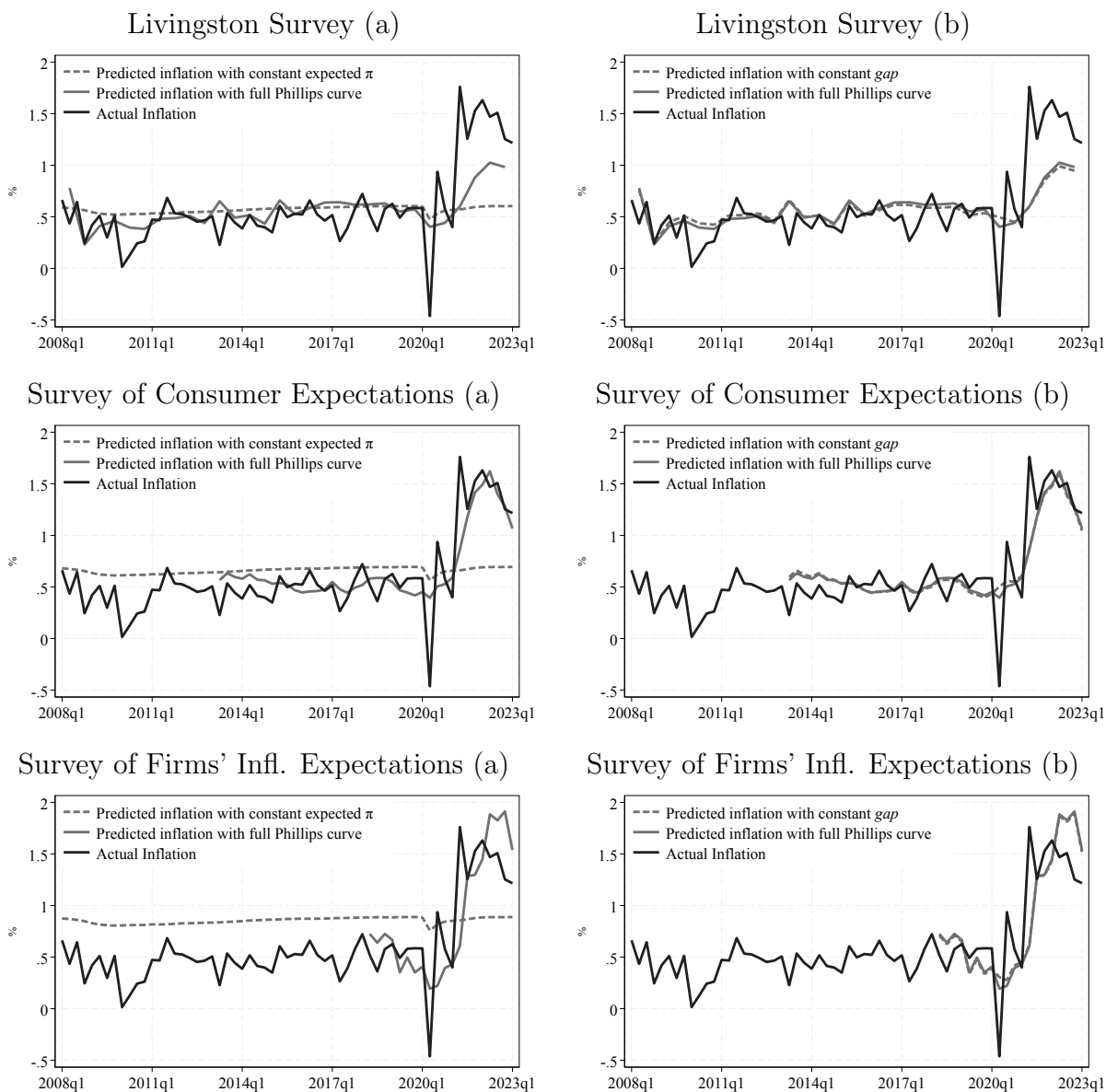
Here we repeat the exercise of Section 1 with various measures of expectations. Key result is that the run-up of inflation expectations can account for inflation increase post-COVID-19 when households or firms survey are used (Survey of Consumer Expectations (New York Fed) or Survey of Firms' Inflation Expectations (Cleveland Fed) or Michigan Survey of Consumers in the main text). The professional forecasts (Cleveland Fed Inflation Expectations, Survey of Professional Forecasters (Philadelphia Fed) or Livingston Survey (Philadelphia Fed)) increase less post-COVID-19, and fail to contribute fully to the increase in actual headline inflation. Note the the baseline Phillips curve (1) is used to do the counterfactual simulations.

Figure B.2: Counterfactual Simulations from the Estimated Phillips Curve, Using Various Measure of Inflation Expectations (a) With inflation expectations at their mean, (b) With gap at its mean



Notes: These counterfactual simulations are done using the baseline Phillips curve (1), using either Cleveland Fed Inflation Expectations or the Survey of Professional Forecasters (Philadelphia Fed) as a measure of expectations.

Figure B.3: Counterfactual Simulations from the Estimated Phillips Curve, Using Various Measure of Inflation Expectations (a) With inflation expectations at their mean, (b) With gap at its mean



Notes: These counterfactual simulations are done using the baseline Phillips curve (1), using either Livingston Survey (Philadelphia Fed), Survey of Consumer Expectations (New York Fed) or Survey of Firms' Inflation Expectations (Cleveland Fed) as a measure of expectations.

Finally, we do a “horse-race” regression to estimate our augmented Phillips curve (2) including both Survey of Professional Forecasters and Michigan Survey of Consumers as potential measures of expected inflation. The results are reported in Table B.1. In column (1) we use *minus* unemployment gap as the measure of the gap and freely estimate it. In column (2) we fix the slope of the negative unemployment gap at the estimate of Hazell, Herreño, Nakamura, and Steinsson [2022] and in column (3) we use the  $\ln V/U$  as the measure of the gap. The results suggest that the Michigan Survey of Consumers is the more relevant measure for expected inflation in the Phillips Curve.<sup>34</sup>

Table B.1: Horse Race using SPF and MSC

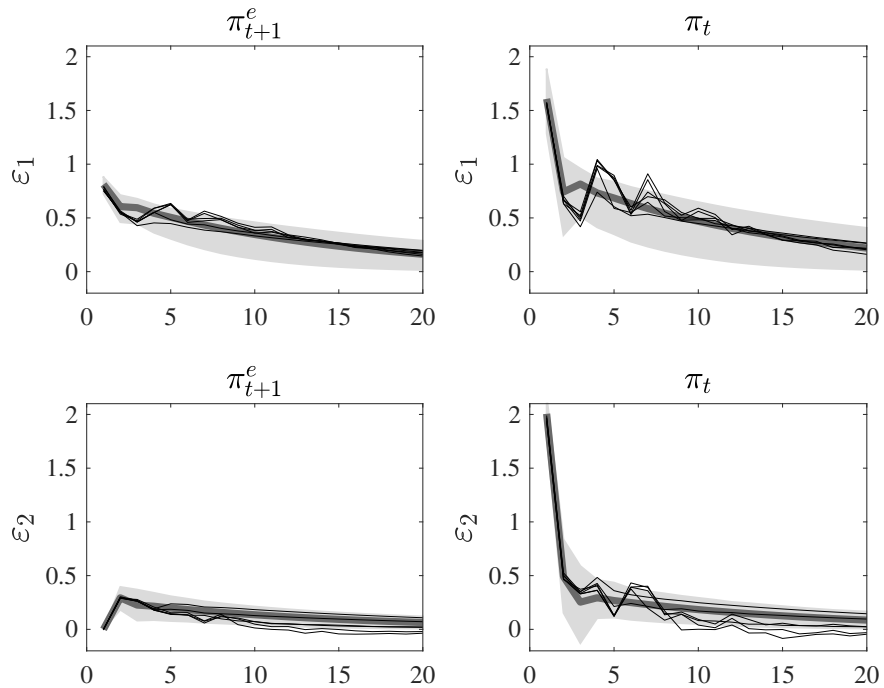
Gap	-ugap or $\ln V/U$		
$\pi$	Sample 1981q3-2007q4		
	(1) -ugap free slope	(2) -ugap fixed slope	(3) $\ln V/U$
MSC	0.40* (0.177)	0.62* (0.161)	0.47* (0.173)
SPF	0.29 (0.272)	-0.02 (0.233)	0.25 (0.267)
$\gamma_g$	0.08* (0.019)	0.0138 (-)	0.19* (0.071)
$\gamma_r$	0.30* (0.082)	0.28* (0.054)	0.24* (0.080)
Observations	106	106	106
J Test (jp)	10.655 (0.979)	11.939 (0.971)	10.636 (0.980)
Weak ID Test	135.594	121.041	39.712

*Notes: this table reports estimates of the augmented Phillips curve (2). All results are using IV-GMM procedure, Newey-West HAC standard errors with six lags are reported in parentheses. The constant term is omitted from the table. The measure of inflation is Core CPI and the gap is measured with minus unemployment gap or  $\log(V/U)$ . All regressors are instrumented using six lags of Romer and Romer’s [2004] shocks (as extended by Wieland and Yang [2020]) and their squares as instruments. A \* indicates significance at 5%. Sample is 1981Q3-2007Q4.*

<sup>34</sup>These findings are in line with the results from Coibion, Gorodnichenko, and Kamdar [2018]. In Coibion and Gorodnichenko [2015b] the authors find that households’ expectations from the Michigan Survey help to explain the missing disinflation puzzle around the 2008 Financial Crisis.

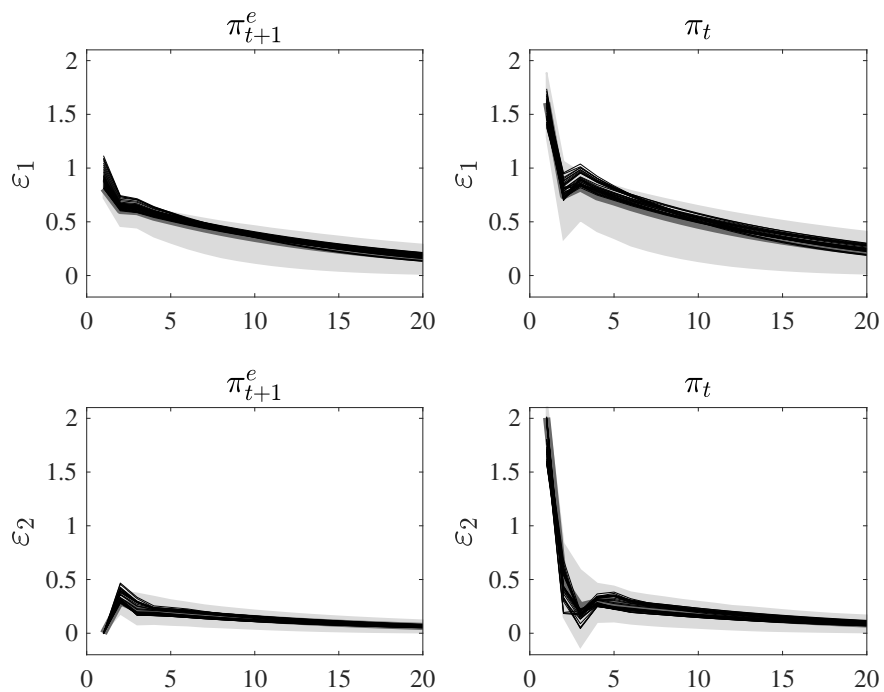
## C Robustness of the 2-VAR to Lags and Sample

Figure C.1: Impulse Responses in the 2-VAR  $(\pi_t, \pi_{t+1}^e)$ , with 2 to 8 Lags



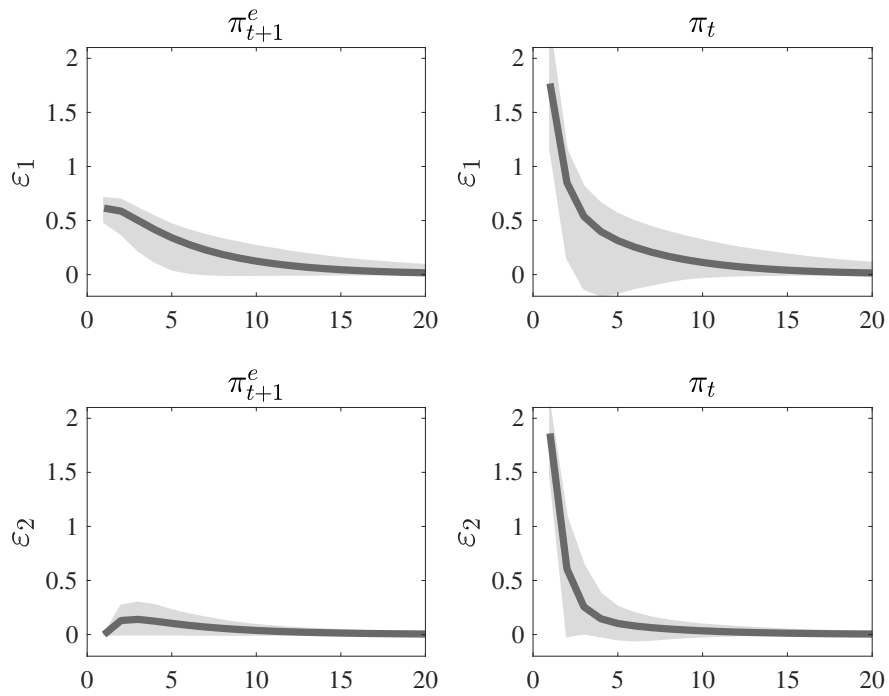
Notes: this Figure plots the impulse responses to a one standard deviation shocks  $\varepsilon_1$  and  $\varepsilon_2$ . These shocks are obtained from a Choleski orthogonalization. The estimated VAR with two lags of Headline CPI inflations and the Michigan Survey of Consumers inflation expectations are in gray. Sample is 1969Q1-2023Q1. Shaded area represents the 95% confidence band. The black lines corresponds to an estimation with 3 to 8 lags.

Figure C.2: Impulse Responses in the 2-VAR  $(\pi_t, \pi_{t+1}^e)$ , Starting with First 20 Years and Adding Years One by One



Notes: this Figure plots the impulse responses to a one standard deviation shocks  $\varepsilon_1$  and  $\varepsilon_2$ . These shocks are obtained from a Choleski orthogonalization. The estimated VAR with two lags of Headline CPI inflations and the Michigan Survey of Consumers inflation expectations are in gray. Sample is 1969Q1-2023Q1. Shaded area represents the 95% confidence band. The black lines corresponds to an estimation samples 1969Q1-1989Q1, 1969Q1-1990Q1, 1969Q1-1991Q1,... etc.

Figure C.3: Impulse Responses in the 2-VAR  $(\pi_t, \pi_{t+1}^e)$  estimated over 2008–2023



Notes: this Figure plots the impulse responses to a one standard deviation shocks  $\varepsilon_1$  and  $\varepsilon_2$ . These shocks are obtained from a Choleski orthogonalization. The estimated VAR with two lags of Headline CPI inflations and the Michigan Survey of Consumers inflation expectations are in gray. Sample is 2008Q1-2023Q1. Shaded area represents the 95% confidence band. The VAR is estimated with one lag.

## D Using Disaggregated Prices

Table D.1 display the 25 expenditures categories we use, as obtained from BLS and used to compute the CPI. Figure D.1 plots sectoral inflations and Table D.2 displays the estimated parameters  $\alpha_i$ ,  $\sigma_i$  and  $\rho$  when we estimate the model

$$\pi_{i,t} = \alpha_i \mathcal{C}_t + e_{i,t},$$

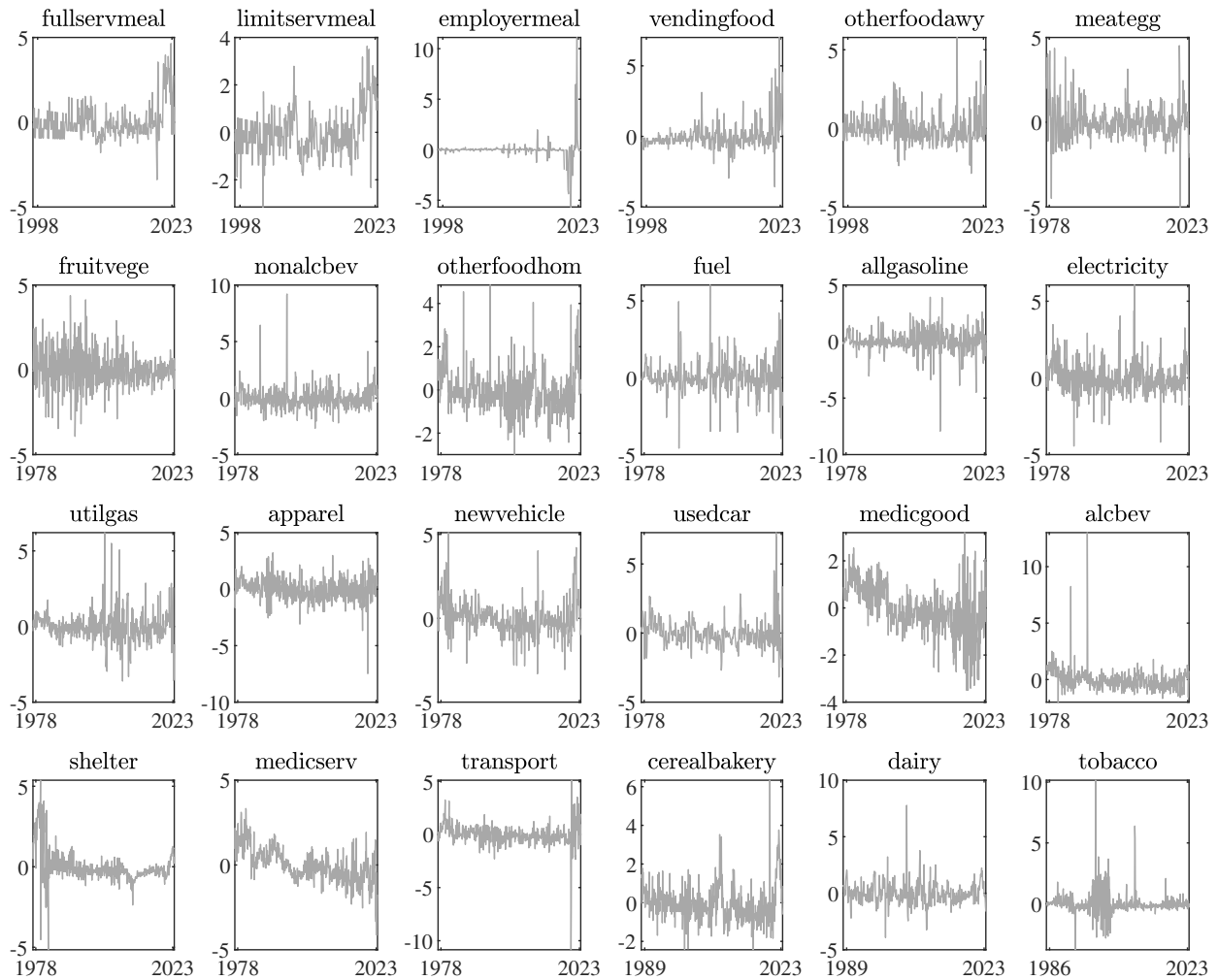
$$\mathcal{C}_t = \rho_C \mathcal{C}_{t-1} + v_t.$$

Table D.1: Summary of Categories

Categories and items	Available sample	Categories and items	Available sample
<b>Food at Home</b>		<b>Food away from Home</b>	
Cereals and bakery products	1990m1-2023m5	Full service meals and snacks	1999m1-2023m5
Meats, poultry, fish, and eggs	1978m1-2023m5	Limited service meals and snacks	1998m12-2023m5
Dairy and related products	1990m1-2023m5	Food at employee sites and schools	1999m1-2023m5
Fruits and vegetables	1978m1-2023m5	Food from vending machines and mobile vendors	1998m12-2023m5
Nonalcoholic beverages and beverage materials	1978m1-2023m5	Other food away from home	1999m1-2023m5
Other food at home	1978m1-2023m5		
<b>Energy commodities</b>		<b>Energy services</b>	
Fuel oil	1978m1-2023m5	Electricity	1978m1-2023m5
Motor fuel (gasoline)	1978m1-2023m5	Utility gas	1978m1-2023m5
<b>less food and energy commodity</b>		<b>less energy services</b>	
Apparel	1978m1-2023m5	Shelter	1978m1-2023m5
New vehicles	1978m1-2023m5	Medical care service	1978m1-2023m5
Used cars and trucks	1978m1-2023m5	Transportation service	1978m1-2023m5
Medical care commodities	1978m1-2023m5		
Alcoholic beverages	1978m1-2023m5		
Tobacco and smoking products	1987m1-2023m5		

*Notes: the main sample starts from 1978m1 due to the availability of the monthly Michigan Survey of Consumers. The disaggregated data are level 3 categories from BLS.*

Figure D.1: Inflation for the Components in the CPI Basket



Notes: this Figure displays the time series of the 25 expenditures categories we use, as obtained from BLS and used to compute the CPI.

Table D.2: Estimated parameters

Parameter	Estimate		Parameter	Estimate	
$\rho$	0.98				
	$\alpha_i$	$\sigma_i$		$\alpha_i$	$\sigma_i$
fullservmeal	0.19	0.73	limitservmeal	0.15	0.84
employermeal	0.05	0.99	vending	0.09	0.94
otherfoodawy	0.06	0.98	meategg	0.04	0.98
fruitvege	0.02	0.99	nonalcohol	0.05	0.97
otherfoodhome	0.10	0.86	fuel	0.03	0.99
gasoline	0.02	1.00	electricity	0.08	0.93
utility gas	0.03	0.99	apparel	0.06	0.96
new vehicle	0.09	0.89	used car	0.03	0.99
medical good	0.09	0.90	alcoholbev	0.08	0.92
shelter	0.13	0.75	medical service	0.11	0.85
transportation	0.08	0.92	cereal bakery	0.16	0.83
dairy product	0.08	0.96	tobacco	0.01	1.00

Notes: we normalize  $\sigma_v = 1$ , and we input series that are normalized (demeaned and standard deviations normalized to 1) because the price series have different volatilities. But the normalization doesn't qualitatively change the results.

## E Average Signal from Disaggregate Price Indices

We show that the signal-extraction problem with multiple disaggregate price indices is equivalent to one with an average signal across these disaggregate indices. The disaggregate signals the agent faces are given by (23). Without loss of generality, consider the  $m$  disaggregate signals the agent uses to form expectations:

$$X_t \equiv \begin{pmatrix} \pi_{1,t} \\ \pi_{2,t} \\ \dots \\ \pi_{m,t} \end{pmatrix} = \ell_m \tilde{z}_t + \begin{pmatrix} \tilde{e}_{1,t} \\ \tilde{e}_{2,t} \\ \dots \\ \tilde{e}_{m,t} \end{pmatrix}, \tag{E.1}$$

with  $\tilde{e}_{j,t} \sim N(0, \tilde{\sigma}_j^2)$ , and where we denote the vector of signals as  $X_t$  and  $\ell_m$  is an  $m \times 1$  vector of ones. Denote the prior of  $\tilde{z}_t$  in  $t - 1$  as:

$$\tilde{z}_t^{prior} \sim N(\tilde{z}_{t|t-1}, \sigma^2), \tag{E.2}$$

where  $\tilde{z}_{t|t-1}$  denotes the prior mean and  $\sigma^2$  the stationary prior variances. The posterior mean of the nowcast is:

$$\tilde{z}_{t|t} = \tilde{z}_{t|t-1} + \kappa_z (X_t - \ell_m \tilde{z}_{t|t-1}), \quad (\text{E.3})$$

where  $\kappa_z$  is the Kalman Gain:

$$\kappa_z = \sigma^2 \ell'_m (\sigma^2 \ell_m \ell'_m + V)^{-1}, \quad (\text{E.4})$$

where  $V$  is a diagonal matrix with entries  $\tilde{\sigma}_j^2$  on the main diagonal. The Kalman Gain can then be explicitly written as a function of  $\sigma^2$  and  $\tilde{\sigma}_j^2$ 's:

$$\begin{aligned} \kappa_z &= \sigma^2 \ell'_m \left( V^{-1} - \frac{V^{-1} \sigma^2 \ell_m \ell'_m V^{-1}}{1 + \sigma^2 \ell'_m V \ell_m} \right) \\ &= \sigma^2 \left[ \begin{pmatrix} \frac{1}{\tilde{\sigma}_1^2} & \frac{1}{\tilde{\sigma}_2^2} & \cdots & \frac{1}{\tilde{\sigma}_m^2} \end{pmatrix} - \begin{pmatrix} \frac{1}{\tilde{\sigma}_1^2} \sum_{j=1}^m \frac{1}{\tilde{\sigma}_j^2} & \frac{1}{\tilde{\sigma}_2^2} \sum_{j=1}^m \frac{1}{\tilde{\sigma}_j^2} & \cdots & \frac{1}{\tilde{\sigma}_m^2} \sum_{j=1}^m \frac{1}{\tilde{\sigma}_j^2} \end{pmatrix} \frac{1}{\frac{1}{\sigma^2} + \sum_{j=1}^m \frac{1}{\tilde{\sigma}_j^2}} \right] \\ &= \begin{pmatrix} \frac{1}{\tilde{\sigma}_1^2} & \frac{1}{\tilde{\sigma}_2^2} & \cdots & \frac{1}{\tilde{\sigma}_m^2} \end{pmatrix} \frac{1}{\frac{1}{\sigma^2} + \sum_{j=1}^m \frac{1}{\tilde{\sigma}_j^2}}. \end{aligned} \quad (\text{E.5})$$

Now consider an average signal:

$$x_t = \tilde{z}_t + \underbrace{\frac{\sum_{j=1}^m \frac{1}{\tilde{\sigma}_j^2} \tilde{e}_{j,t}}{\sum_{j=1}^m \frac{1}{\tilde{\sigma}_j^2}}}_{\equiv \epsilon_t}, \quad (\text{E.6})$$

$$\epsilon_t \sim N\left(0, \underbrace{\frac{1}{\sum_{j=1}^m \frac{1}{\tilde{\sigma}_j^2}}}_{\equiv \sigma_\epsilon^2}\right). \quad (\text{E.7})$$

With the same prior, the Kalman Gain is given by:

$$\hat{\kappa}_z = \frac{\frac{1}{\sigma_\epsilon^2}}{\frac{1}{\sigma^2} + \frac{1}{\sigma_\epsilon^2}}. \quad (\text{E.8})$$

Using (E.5) and (E.8), it is then straightforward to show that the posterior mean  $\tilde{z}_{t|t}$  is the same when the agent uses disaggregate signals (E.1) with the aggregate signal (E.6).

Moreover, the stationary posterior variances are the same as well. As a result, the stationary posterior belief formed by observing multiple signals (E.1) is equivalent to one formed using an average signal (E.6).

Now consider the actual disaggregate signals from (19) and the perceived disaggregate signals from (23). Apply our results above, the average signals are given by:

$$s_t = \sum_{j \in S} \frac{1/\tilde{\sigma}_j^2}{\underbrace{\sum_{j \in S} 1/\tilde{\sigma}_j^2}_{\equiv \chi_j}} \pi_{j,t} = \beta \pi_{t+1}^e + \gamma_g \text{gap}_t + \underbrace{\sum_{j \in S} \chi_j e_{j,t}}_{\equiv \epsilon_t} \quad (\text{Average Signal ALM})$$

$$s_t = \sum_{j \in S} \frac{1/\tilde{\sigma}_j^2}{\underbrace{\sum_{j \in S} 1/\tilde{\sigma}_j^2}_{\equiv \chi_j}} \pi_{j,t} = \tilde{z}_t + \underbrace{\sum_{j \in S} \chi_j \tilde{e}_{j,t}}_{\equiv \tilde{\epsilon}_t} \quad (\text{Average Signal PLM})$$

These give the first equations in (27) and (26), where

$$\sigma_\epsilon^2 = \sum_{j \in S} \chi_j^2 \sigma_j^2, \quad \tilde{\sigma}_\epsilon^2 = \sum_{j \in S} \chi_j^2 \tilde{\sigma}_j^2 = \frac{1}{\sum_{j \in S} \frac{1}{\tilde{\sigma}_j^2}} \quad (\text{E.9})$$

Given the actual and perceived aggregate supply shocks  $\eta_t = \sum_{j=1}^N \omega_j e_{j,t}$  and  $\tilde{\eta}_t = \sum_{j=1}^N \omega_j \tilde{e}_{j,t}$ , we can also derive the actual and perceived correlation between  $\epsilon_t$  and  $\eta_t$  ( $\tilde{\epsilon}_t$  and  $\tilde{\eta}_t$ ):

$$\rho \equiv \text{corr}(\epsilon_t, \eta_t) = \frac{\sum_{j \in S} \chi_j \omega_j \sigma_j^2}{\sigma_\epsilon \sigma_\eta}, \quad \tilde{\rho} \equiv \text{corr}(\tilde{\epsilon}_t, \tilde{\eta}_t) = \frac{\sum_{j \in S} \chi_j \omega_j \tilde{\sigma}_j^2}{\tilde{\sigma}_\epsilon \tilde{\sigma}_\eta} \quad (\text{E.10})$$

## F Models with Rational Expectations

### F.1 Incomplete Information Rational Expectations

Take the IIRE model described by (9)-(12). The agent forms expectations about  $\text{gap}_t$ .

Denoting the nowcasts of which as  $\text{gap}_{t|t}$ , expectations are given by:

$$\begin{aligned} E_t[\pi_{t+1}] &= E_t[\beta E_{t+1}\pi_{t+2} + \gamma_g \text{gap}_{t+1} + e_{t+1}] \\ &= \frac{\gamma_g \rho}{1 - \beta \rho} \text{gap}_{t|t}. \end{aligned} \tag{F.1}$$

The nowcast  $\text{gap}_{t|t}$  is given by:<sup>35</sup>

$$\text{gap}_{t|t} = \text{gap}_{t|t-1} + k_i (s_t - \gamma_g \text{gap}_{t|t-1}), \tag{F.2}$$

$$\mathcal{K} = \sigma_k^2 \gamma_g (\gamma_g^2 \sigma_k^2 + \sigma_\epsilon^2)^{-1}, \tag{F.3}$$

$$\sigma_k^2 = \rho^2 (\sigma_k^2 - \mathcal{K} \gamma_g \sigma_k^2) + \sigma_v^2, \tag{F.4}$$

where  $\mathcal{K}$  is the stationary Kalman Gain and  $\sigma_k^2$  is the stationary posterior variance. This leads to equations (13) and (14) in the main text. Note that as  $\sigma_\epsilon \rightarrow 0$ ,  $\mathcal{K} \rightarrow 1/\gamma_g$  and  $w_t \rightarrow e_t$ . The IIRE case converges to the FIRE case.

### F.2 Hybrid Phillips Curve or Adaptive Expectations

One related question is whether a hybrid Phillips Curve or adaptive expectations can help to explain the joint dynamics between expected and actual inflation. We consider a Phillips

---

<sup>35</sup>Note in (F.3) the agent uses correct  $\sigma_\epsilon$  because when the agent is rational, she can easily back-out the correct  $\rho$ ,  $\gamma_g \sigma_v$  and  $\sigma_\epsilon$  with the variance-covariance structure of  $s_t$ . As a result, the agent's information will not support any subjective  $\tilde{\sigma}_\epsilon \neq \sigma_\epsilon$ .

Curve taking the following hybrid form:

$$\pi_t = \beta \underbrace{\left( \tau \pi_{t-1} + (1 - \tau) E_t^{FIRE} \pi_{t+1} \right)}_{\text{observed in MSC}} + \gamma_g \text{gap}_t + e_t, \quad (\text{F.5})$$

$$\text{gap}_t = \rho \text{gap}_{t-1} + v_t, \quad (\text{F.6})$$

where  $\tau$  can represents the indexation, the fraction of people using adaptive expectations, or motivated by k-level thinking as in Beaudry, Carter, and Lahiri [2023]. The expectations formed under FIRE takes into account that there are backward looking component in inflation. It is easy to show that inflation takes the following form using undetermined coefficients:

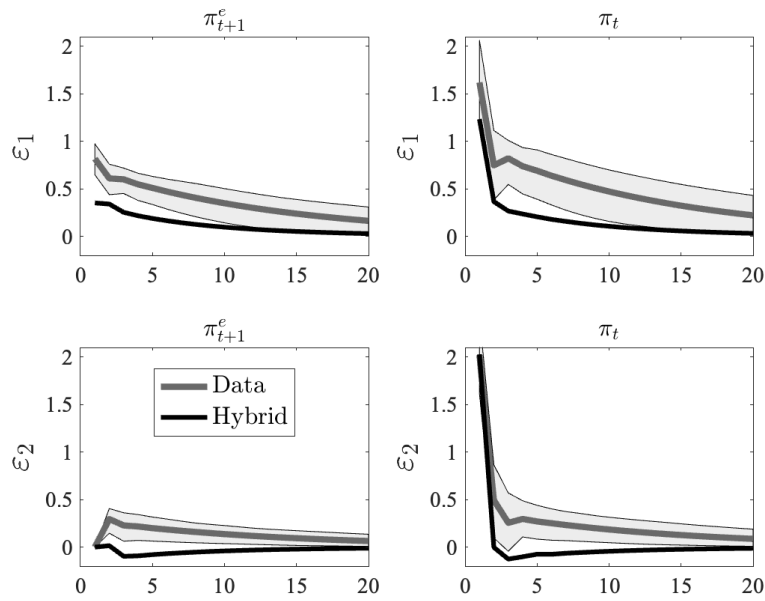
$$\pi_t = a\pi_{t-1} + b\text{gap}_t + ce_t, \quad (\text{F.7})$$

with

$$\begin{cases} a &= \frac{\beta\tau}{1-a\beta(1-\tau)}, \\ b &= \frac{\beta(1-\tau)b\rho+\gamma_g}{1-a\beta(1-\tau)}, \\ c &= \frac{1}{1-a\beta(1-\tau)}. \end{cases}$$

Following our approach in section 2.2, we set  $\beta$ ,  $\rho$ ,  $\sigma_v$  and  $\gamma_g$  at values consistent with our Phillips Curve, and we estimate the free parameter  $\tau$  to match the IRFs from the bivariate VAR(2). Our estimate is  $\hat{\tau} = 0.05$ , and the above model cannot match the empirical IRFs well:

Figure F.1: The Joint Process of  $\pi$  and  $\pi_{t+1}^e$  in the Data and Under Models with Rational Expectations

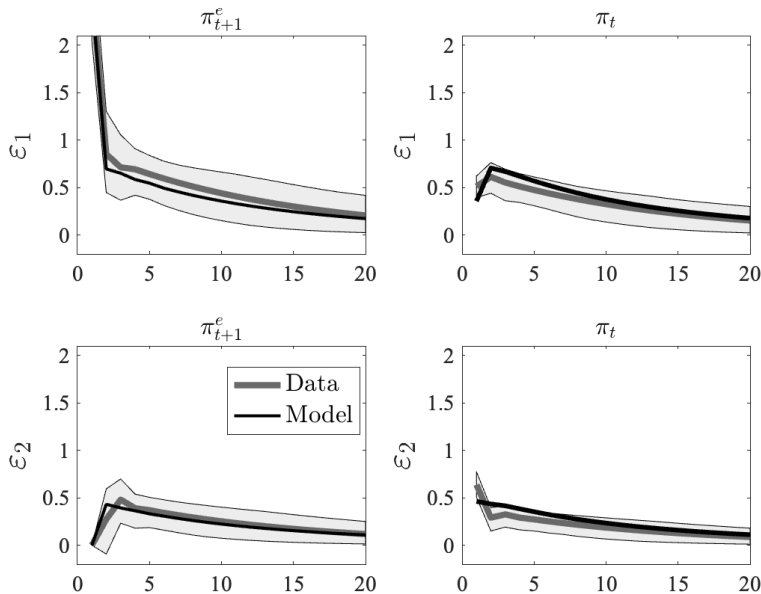


Notes: on this Figure, the grey line plots the impulse responses to a one standard deviation shocks  $\varepsilon_1$  and  $\varepsilon_2$  estimated with data from the Michigan Survey of Consumers and Headline CPI. Sample is 1969Q1-2023Q1. Shaded area represents the 95% confidence band. The black line plot the average impulse responses (over 200 simulations of length 216) obtained from the same VAR estimated on simulated data, when the Data Generating Process is the estimated hybrid model (F.5).

## G Alternative Order of Cholesky VAR

We present the IRFs from Cholesky VAR(2) where we order headline inflation first and expected inflation the second. This change of ordering reflects an alternative identification assumption that the first underlying shock affects  $\pi_t$  and  $\pi_{t+1}^e$  simultaneously and the second shock affects  $\pi_{t+1}^e$  on impact then  $\pi_t$  with a lag. Note our Cholesky VAR is just method to summarize joint dynamics of inflation and expectations. If our model is close to the true data generating process for inflation and expected inflation, we would expect IRF from this VAR with alternative (but possibly incorrect) ordering to have similar result. Figure G.1 shows the results from this exercise. Our model matches very well with the VAR using alternative ordering.

Figure G.1: IRF from data and model simulation



*Notes: thick gray line is IRF from bi-VAR with actual data; marked black line is average IRF from simulated data across 200 random samples. The estimated VAR is VAR(2) with Cholesky Decomposition ordering  $\pi_t$  -  $\pi_{t+1}^e$ . The shaded area represents 95% CI.*

# H State-space Representation of Model

## H.1 Model

For easy exposition, we derive the state-space representation of our model with the orthogonalized residual supply shock  $w_t$  defined in section 4.3. To save notations, we define

$$\omega = \varrho \frac{\sigma_\eta}{\sigma_\epsilon} \quad (\text{H.1})$$

According to (45),  $w_t$  is given by:

$$w_t = \eta_t - \omega \epsilon_t \quad (\text{H.2})$$

The two observables  $\pi_{t+1|t,0}$  and  $\pi_t$  can be written as system of equations of latent states  $\tilde{z}_{t|t-1,1}$  and  $\text{gap}_t$ .

$$\begin{aligned} \pi_{t+1|t,0} &= \tilde{\rho}_z \tilde{z}_{t|t,0} = \tilde{\rho}_z ((1-K)\tilde{z}_{t|t-1,1} + K s_t) \\ &= \tilde{\rho}_z ((1-K)\tilde{z}_{t|t-1,1} + K(\beta\pi_{t+1|t,0} + \gamma_g \text{gap}_t + \epsilon_t)) \\ &= \frac{\tilde{\rho}_z(1-K)}{1-K\beta\tilde{\rho}_z} \tilde{z}_{t|t-1,1} + \frac{\tilde{\rho}_z K \gamma_g}{1-K\beta\tilde{\rho}_z} \text{gap}_t + \frac{\tilde{\rho}_z K}{1-K\beta\tilde{\rho}_z} \epsilon_t. \end{aligned} \quad (\text{H.3})$$

From (27):

$$\begin{aligned} s_t &= \pi_{t+1|t,0} + \gamma_g \text{gap}_t + \epsilon_t \\ &= \frac{\beta\tilde{\rho}_z(1-K)}{1-K\beta\tilde{\rho}_z} \tilde{z}_{t|t-1,1} + \frac{\gamma_g}{1-K\beta\tilde{\rho}_z} \text{gap}_t + \frac{1}{1-K\beta\tilde{\rho}_z} \epsilon_t. \end{aligned} \quad (\text{H.4})$$

Inflation is given by:

$$\begin{aligned} \pi_t &= \beta\pi_{t+1|t,0} + \gamma_g \text{gap}_t + \omega \epsilon_t + w_t \\ &= \frac{\beta\tilde{\rho}_z(1-K)}{1-K\beta\tilde{\rho}_z} \tilde{z}_{t|t-1,1} + \frac{\gamma_g}{1-K\beta\tilde{\rho}_z} \text{gap}_t + \left( \frac{K\beta\tilde{\rho}_z}{1-K\beta\tilde{\rho}_z} + \omega \right) \epsilon_t + w_t. \end{aligned} \quad (\text{H.5})$$

From (33) and expression of  $s_t$ , we get recursion of  $\tilde{z}_{t|t-1,1}$ :

$$\begin{aligned}
\tilde{z}_{t+1|t,1} &= \tilde{\rho}_z \tilde{z}_{t|t,1} = \tilde{\rho}_z (1 - K - k) \tilde{z}_{t|t-1,1} + \tilde{\rho}_z K s_t + \tilde{\rho}_z k \pi_t \\
&= \tilde{\rho}_z \left( 1 - (K + k) \frac{1 - \beta \tilde{\rho}_z}{1 - K \beta \tilde{\rho}_z} \right) \tilde{z}_{t|t-1,1} + \tilde{\rho}_z \frac{(K + k) \gamma_g}{1 - K \beta \tilde{\rho}_z} \text{gap}_t \\
&\quad + \tilde{\rho}_z \left( \frac{K + \tilde{\rho}_z K k \beta}{1 - K \beta \tilde{\rho}_z} + \omega k \right) \epsilon_t + \tilde{\rho}_z k w_t.
\end{aligned} \tag{H.6}$$

We could write the state-space representation as:

$$X_t \equiv \begin{pmatrix} \pi_{t+1|t,0} \\ \pi_t \\ \tilde{z}_{t+1|t,1} \\ \text{gap}_t \end{pmatrix} = F X_{t-1} + B \begin{pmatrix} \epsilon_t \\ w_t \\ v_t \end{pmatrix}, \tag{H.7}$$

where

$$F = \begin{pmatrix} 0 & 0 & \frac{\tilde{\rho}_z(1-K)}{1-K\beta\tilde{\rho}_z} & \rho \frac{\tilde{\rho}_z K \gamma_g}{1-K\beta\tilde{\rho}_z} \\ 0 & 0 & \frac{\beta\tilde{\rho}_z(1-K)}{1-K\beta\tilde{\rho}_z} & \rho \frac{\gamma_g}{1-K\beta\tilde{\rho}_z} \\ 0 & 0 & \tilde{\rho}_z \left( 1 - (K + k) \frac{1 - \beta \tilde{\rho}_z}{1 - K \beta \tilde{\rho}_z} \right) & \tilde{\rho}_z \frac{(K+k)\gamma_g}{1-K\beta\tilde{\rho}_z} \rho \\ 0 & 0 & 0 & \rho \end{pmatrix}, \tag{H.8}$$

$$B = \begin{pmatrix} \frac{\tilde{\rho}_z K}{1-K\beta\tilde{\rho}_z} & 0 & \frac{\tilde{\rho}_z K \gamma_g}{1-K\beta\tilde{\rho}_z} \\ \frac{K\beta\tilde{\rho}_z}{1-K\beta\tilde{\rho}_z} + \omega & 1 & \frac{\gamma_g}{1-K\beta\tilde{\rho}_z} \\ \left( \frac{K + \tilde{\rho}_z K k \beta}{1 - K \beta \tilde{\rho}_z} + \omega k \right) \tilde{\rho}_z & \tilde{\rho}_z k & \tilde{\rho}_z \frac{(K+k)\gamma_g}{1-K\beta\tilde{\rho}_z} \\ 0 & 0 & 1 \end{pmatrix}. \tag{H.9}$$

The observational equation is given by:

$$O_t = \begin{pmatrix} I_{2 \times 2} & \mathbf{0}_{2 \times 2} \\ \mathbf{0}_{2 \times 2} & \mathbf{0}_{2 \times 2} \end{pmatrix} X_t. \tag{H.10}$$

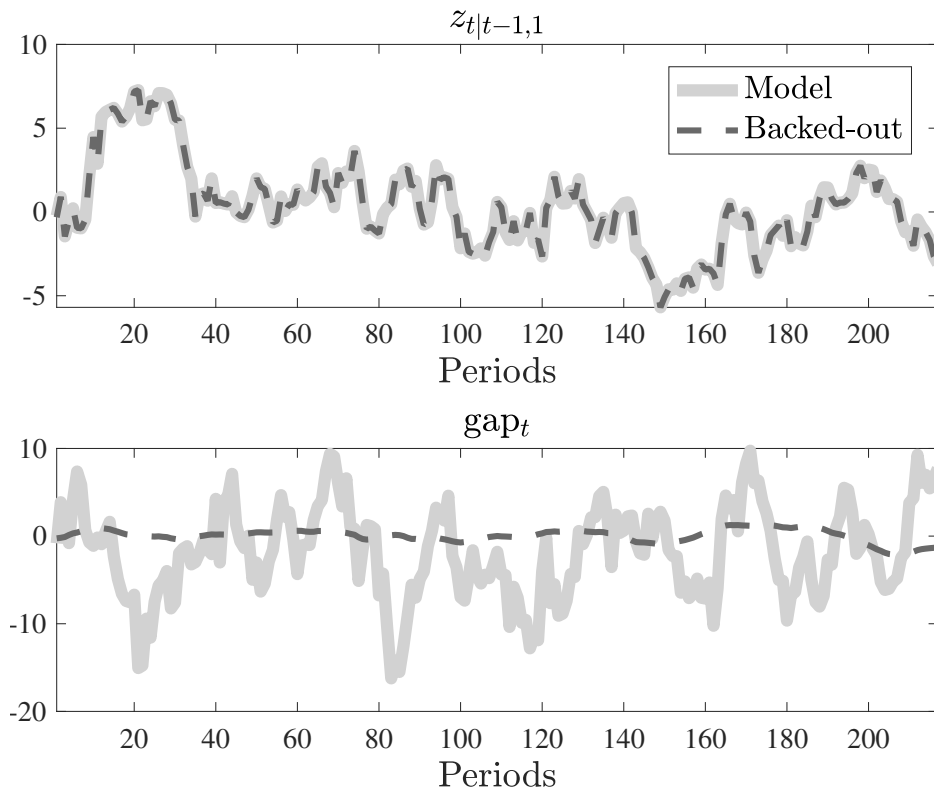
We can then estimate the hidden states  $\tilde{z}_{t|t-1,1}$  and  $\text{gap}_t$  using Kalman Filter Smoothing, then get the corresponding shocks implied by the state-space representation.

The precision of the estimated states and shocks depend on the parameters in  $F$  and  $B$ .

To illustrate the performance of this approach in the context of our estimated model, we

simulate data using parameters from Table 4. We then plot the time series of the estimated states  $E_t\pi_{t+1}$ ,  $\pi_t$ ,  $\tilde{z}_{t|t-1}$  and  $\text{gap}_t$  in Figure H.1. The blue solid lines are the actual hidden states from simulated data and the red dash lines are the estimated ones from the above approach. Not surprisingly, the hidden state  $\tilde{z}_{t|t-1}$  is very well recovered where the estimated values are almost identical to the actual ones. Whereas the  $\text{gap}_t$  is very illy recovered. This is because the observables  $\{E_t\pi_{t+1}, \pi_t\}$  contain a lot more information for  $\tilde{z}_{t|t-1}$  and almost no information about  $\text{gap}_t$  due to the fact  $\gamma_g$  is very small in the actual DGP. As a result, the Kalman Smoothing algorithm puts low weights on the observables when making predictions about this hidden state. Figure H.2 depicts the backed-out shocks and compares them with

Figure H.1: Estimated v.s. actual latent states  $\tilde{z}_{t|t-1}$  and  $\text{gap}_t$  from simulated data

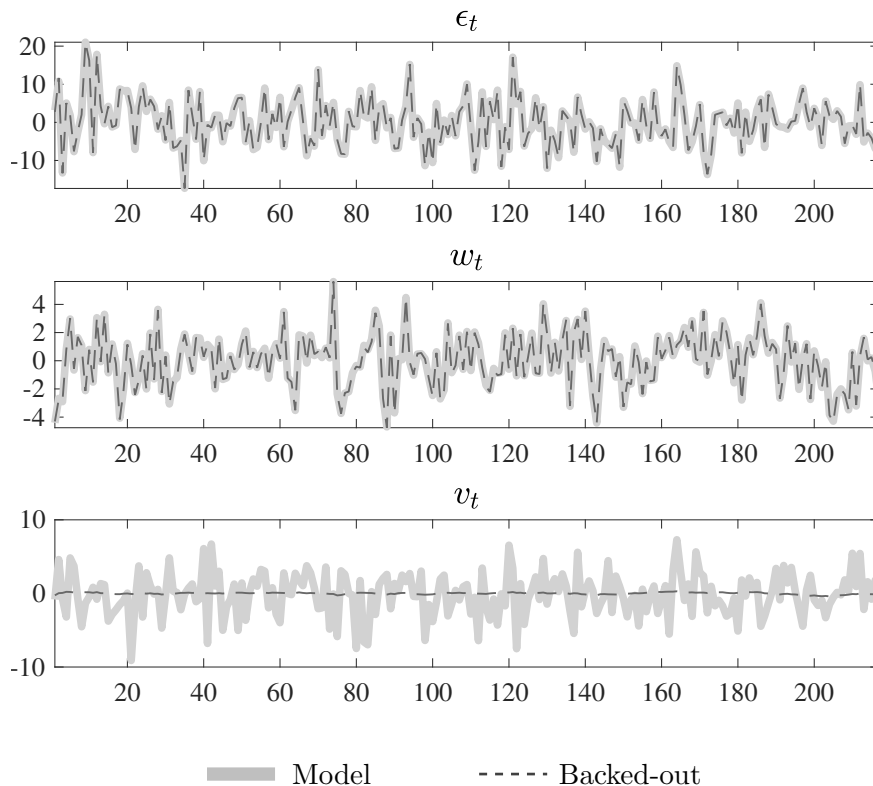


*Notes: the blue solid lines are actual latent states from simulated data. The red dash lines are the recovered latent states using the Kalman Smoothing.*

actual shock series simulated. For the same reason as the latent states, the observations are quite informative about the broad-based shocks  $\epsilon_t$  and the aggregate shock  $w_t$ , but they are

not informative about the common shock  $v_t$ . As a result, the recovered  $v_t$  series are much less volatile and not really comparable to the actual shock series.

Figure H.2: Estimated v.s. actual latent states  $\tilde{z}_{t|t-1,1}$  and  $\text{gap}_t$  from simulated data

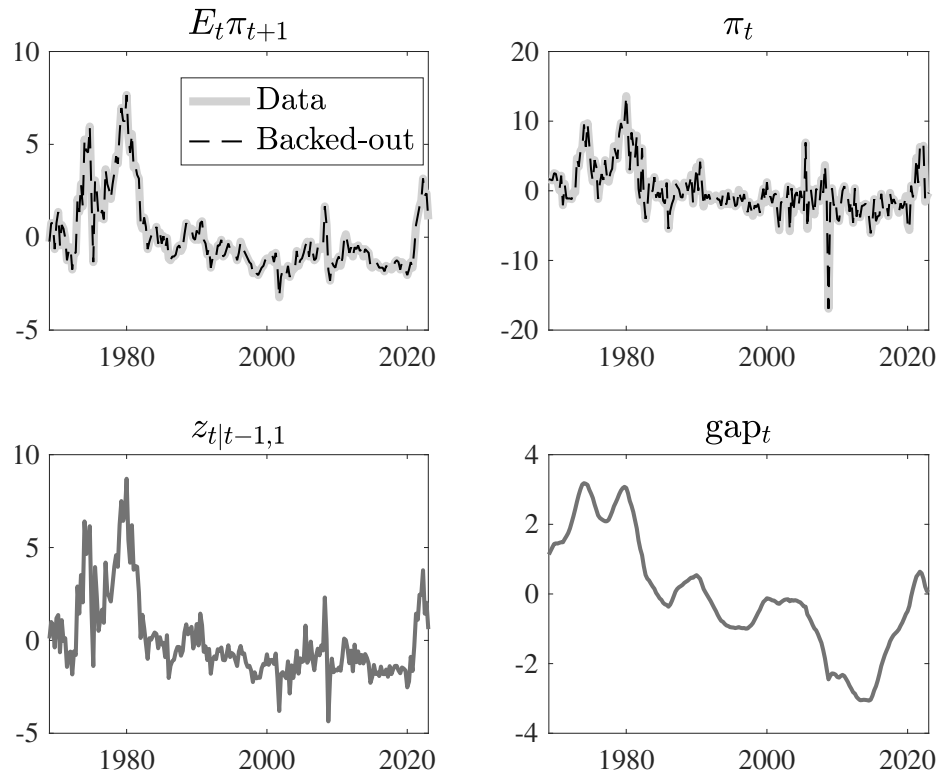


Notes: the dark gray lines are model simulated latent states. The light gray lines are the recovered latent states using the Kalman Smoothing.

## H.2 Backed-out Series from Real Data

The figure H.3 depicts the recovered states  $\{E_t\pi_{t+1}, \pi_t, \tilde{z}_{t|t-1,1}, \text{gap}_t\}$  applying Kalman Smoothing. By construction, the expected inflation and aggregate inflation are observable so they coincide with each other. Because the actual values for  $\tilde{z}_{t|t-1,1}$  and  $\text{gap}_t$  are treated as unobserved, there are no corresponding actual values plotted for these two variables.

Figure H.3: Estimated v.s. actual states from actual data



Notes: the states  $\pi_t$  and  $E_t \pi_{t+1}$  are observables. In the two upper panels, the thick grey line plots actual states and the black dashed line is the recovered latent states using the Kalman Smoothing. The two lines coincide by construction as these two states are observable. Because the actual values for  $\tilde{z}_{t|t-1,1}$  and  $gap_t$  are treated as unobserved, there are no corresponding actual values plotted for these two variables.

# I The Baseline Model without the Timing Restriction

In this appendix, we reestimate the model under the assumption that inflation expectations are reported *after* observing current inflation, meaning that  $\pi_{t+1}^e = \pi_{t+1|t,1}$ . The estimated parameters become:

Table I.1: Estimated parameters

From the Phillips Curve			
$\beta$	0.99	$\rho$	0.89
$\sigma_v$	3.02	$\gamma_g$	0.0138
$\sigma_\eta$	2.24		
From Minimum Distance			
$\tilde{\sigma}_z$	0.45	$\sigma_\epsilon$	2.80
$\tilde{\rho}_z$	0.98	$\tilde{\sigma}_w$	2.46
$\varrho$	0.08	$\tilde{\sigma}_\epsilon$	1.58
$\tilde{\varrho}$	0.00		

Notes: The Phillips curve estimates use the baseline estimation with Hazell, Herreño, Nakamura, and Steinson's [2022] estimate of  $\gamma_g$ .  $\sigma_\eta$  is implied by the variance of the residual  $e$  from the Phillips curve.

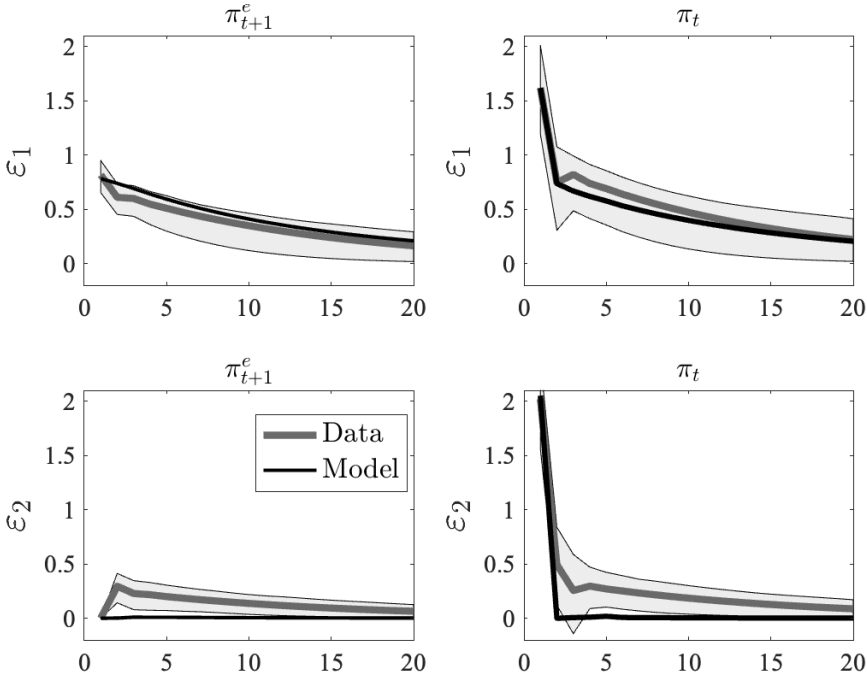
In Figure I.1, we see the model cannot match the IRF of the second shock in the Cholesky VAR because the shock  $w_t$  affecting  $\pi_t$  on impact will have no impact on expectations at all in the model without timing restriction. The variance-covariance structure from the model without timing restriction is:

Table I.2: Variance and Auto-covariance of Inflation

	Data	PLM	Model
$var(\pi_{t,h})$	12.52	11.14	11.14
$cov(\pi_{t,h}, \pi_{t-1,h})$	7.70	5.11	4.98
$cov(\pi_{t,h}, \pi_{t-2,h})$	6.99	4.74	4.87

Notes: PLM stands for "Perceived Law of Motion". The PLM and "Model" moments are the average moment across 200 random samples. In the estimations, we penalize distance between data and model 2-VAR responses as well as distance between these three moments in the PLM and in the model.

Figure I.1: IRF from data and simulated data from model without timing restriction



Notes: The thick gray line is the IRF from the 2-VAR with actual data; the black line is the average IRF from simulated data across 200 random samples. The estimated VAR is a VAR(2) with Cholesky decomposition, ordering  $\pi_{t+1}^e$  first. The shaded area represents the 95% confidence interval.